# Formation and Decomposition of Iron–Carbon σ-Bonds in the Reaction of Iron(II)–Poly(amino carboxylate) Complexes with CO2- Free Radicals. A Pulse Radiolysis Study

**Sara Goldstein,**[*,†] **Gidon Czapski,**[†] **Haim Cohen,**[*,‡,§] **and Dan Meyerstein**[§,||]

*Contribution from the Department of Physical Chemistry, The Hebrew University of Jerusalem, Jerusalem 91904, Israel, Nuclear Research Centre Negev, Beer-Sheva, Israel, and R. Bloch Coal Research Center and Department of Chemistry, Ben-Gurion University of the Negev, Beer-Sheva, Israel. Received September 18, 1987*

**Abstract:** The reactions of ferrous poly(amino carboxylate) complexes with $CO_2^-$ were studied at neutral pH in aqueous solutions. The results indicate that complexes with metal–carbon σ-bonds are formed as unstable intermediates with maximum absorption bands at 405 nm ($\epsilon = 620 \pm 50$ $M^{-1}$ $cm^{-1}$) and at 420 nm ($\epsilon = 950 \pm 100$ $M^{-1}$ $cm^{-1}$) for the NTA and HEDTA complexes, respectively. The transient complexes are in equilibrium with the ferrous poly(amino carboxylate) complex and $CO_2^-$ free radical. The stability constants for the complexes of $CO_2^-$ with ferrous NTA and HEDTA complexes were determined to be larger than $10^5$ $M^{-1}$. The kinetics of formation and decomposition and possible reaction mechanisms for these intermediates are discussed. We determined the specific rate constants for the formation of the iron–carbon σ-bonds ($1.5 \times 10^7$ and $6.2 \times 10^6$ $M^{-1}$ $s^{-1}$ for NTA and HEDTA, respectively) as well as for the homolytic cleavage of the metal–carbon bond (140 and 25 $s^{-1}$ for NTA and HEDTA, respectively). It is shown that the ferrous poly(amino carboxylate) complexes induce the disproportionation of the $CO_2^-$ free radicals to form CO and $CO_2$ via $CO_2^- + L-Fe^{III}CO_2^{2-}$ with specific rate constants of $1.9 \times 10^7$ and $4.5 \times 10^6$ $M^{-1}$ $s^{-1}$ for L = NTA and HEDTA, respectively.

Complexes containing metal–carbon σ-bonds are important intermediates in a wide variety of catalytic, synthetic, and biochemical processes.[1] In many systems the decomposition reactions of these bonds involve homolytic or heterolytic dissociation of the metal–carbon bond.[2] It has been well established that transition-metal ions and their complexes enhance damage caused by free radicals in biological systems. Such damage is initiated by ionizing radiation, drugs (e.g. bleomycin), and herbicides (e.g. paraquat). Similar processes occur in phagocytosis and pathological processes (e.g. anoxia and heart or brain events).[3] In most of these systems, $O_2^-$, an aliphatic free radical, or a reducing agent initiates the metal-catalyzed reaction, where OH· radicals are assumed to be formed and are assumed to be responsible for the biological damage. If OH· is formed, then a secondary aliphatic free radical (R·) is formed due to the reactivity of hydroxyl radicals with organic scavengers (RH) via reaction 1. It is believed that

$$OH· + RH \rightarrow H_2O + R· \qquad (1)$$
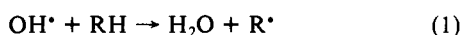
some of the DNA and membrane damage is caused through the reaction with either the OH· radical or the aliphatic radical. This damage may take place through the site-specific mechanism, where the metal is bound to the biological target, and the relevant reactions, involving OH· or R·, occur at or in the vicinity of the binding site and not randomly.[3]

The formation of complexes with metal–carbon σ-bonds of the type $L_mM^n$–R (where L is a ligand and R an alkyl group) has been reported for $M^n = Ni^{II}$, $Cu^{II}$, $Cu^{III}$, $Mn^{III}$, $Fe^{III}$, $Cr^{III}$, $Co^{III}$, $Cd^{II}$, $Hg^{II}$, and $Ti^{IV}$.[1,4] The formal oxidation state of the metal center in the complex is calculated assuming that the alkyl residue R is a carbanion ligand. Nevertheless, the bond must have some covalent nature as carbanions are expected to be extremely unstable in aqueous solutions.

Iron(II) compounds are of major importance in many biological systems. These compounds are capable in some of these systems to form OH· radicals via the Fenton reaction[3] (eq 2).

$$Fe^{II} + H_2O_2 \rightarrow Fe^{III} + OH^- + OH· \qquad (2)$$
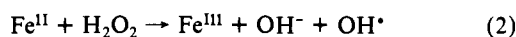
We have chosen to study the formation of the metal–carbon bond formed in the reaction of ferrous complexes of nitrilotri-

acetate (NTA) and N-(hydroxyethyl)ethylenediaminetriacetate (HEDTA) with the highly reducing $CO_2^-$ radical anion ($E°$-$(CO_2/CO_2^-) = -1.84$ V),[5] using the pulse radiolysis technique. These and other complexes of iron with poly(amino carboxylates) are often used as models for biological targets as they contain amine and carboxylate, which are common donor groups in biomolecules and also have available coordination sites.

Our study may also have some implication to a recent report[6] concerning the mechanism of the reaction of $Fe^{II}HEDTA$ with $H_2O_2$. In this study it was suggested that this Fenton-like reaction (reaction 2) generates a metal–peroxo intermediate ($Fe^{II}H_2O_2$) rather than an OH· radical. It was further suggested that this metal–peroxo complex forms a ternary complex with a formate ion, which decomposes to yield $Fe^{II}HEDTA·$ ligand radical, and subsequently this radical dimerizes and causes degradation of the ligand. We suggest, and intend to prove through this study, that either a metal–peroxo complex or an OH· radical can be formed in this Fenton-type reaction. OH· radicals abstract H atoms from $HCO_2^-$ yielding $CO_2^-$, and it is possible that the metal–peroxo complex does the same abstraction. Subsequently, $CO_2^-$ reacts with $Fe^{II}HEDTA$ to form a complex with a metal–carbon σ-bond ($HEDTA-Fe^{III}CO_2^{2-}$), which is the intermediate observed by Rush and Koppenol[6] and was wrongly identified as the $Fe^{II}HEDTA·$ ligand radical. Therefore, through performing such experiments, one cannot distinguish between the species formed in such Fenton-type reactions.

## Experimental Section

**Materials.** All the compounds were of analytical grade and were used without further purification: nitrilotriacetate, ferrous sulfate, sodium formate, and ferrous and ferric ammonium sulfate were supplied by E. Merck, HEDTA was supplied by Sigma, and cobalt hexaammine chlo-

---

[†] The Hebrew University of Jerusalem.
[‡] Nuclear Research Centre Negev.
[§] R. Bloch Coal Research Center, Ben-Gurion University of the Negev.
[||] Department of Chemistry, Ben-Gurion University of the Negev.

(1) (a) Halpern, J. H. *Pure Appl. Chem.* **1983,** *55,* 1059. (b) Halpern, J. *Ibid.* **1986,** *58,* 575. (c) Halpern, J. *Acc. Chem. Res.* **1983,** *15,* 238.
(2) Espenson, J. H. In *Advances in Inorganic and Bioinorganic Mechanisms;* Sykes, A. J., Ed.; Academic: London, 1982; Vol. II.
(3) Goldstein, S.; Czapski, G. *J. Free Radical J. Biol. Med.* **1986,** *2,* 3, and references cited therein.
(4) (a) Cohen, H.; Meyerstein, D. *Inorg. Biochem.* **1974,** *13,* 2434. (b) Freiberg, M.; Mulac, W. A.; Meyerstein, D. *J. Chem. Soc., Faraday Trans. 1* **1980,** *76,* 1838. (c) Freiberg, M.; Mulac, W.; Meyerstein, D. *Ibid.* **1980,** *76,* 1825. (d) Sorek, Y.; Cohen, H.; Mulac, W. H.; Schmidt, K. H.; Meyerstein, D. *Inorg. Chem.* **1983,** *22,* 3040. (e) Sorek, Y.; Cohen, H.; Meyerstein, D. *J. Chem. Soc., Faraday Trans. 1* **1985,** *81,* 233.
(5) Koppenol, W. H.; Rush, J. D. *J. Phys. Chem.* **1987,** *91,* 4429.
(6) Rush, J. D.; Koppenol, W. H. *J. Inorg. Biochem.* **1987,** *29,* 199.

ride was supplied by K & K. All solutions were prepared with distilled water, which was further purified with a Millipore setup. Solutions of ferrous and ferric complexes of NTA and HEDTA were prepared by adding the solid iron salt to $N_2O$-saturated solutions containing the ligand and formate, with the syringes technique. The pH was adjusted to 7 by adding $N_2O$-saturated solutions of $HClO_4$ or $NaOH$ as required.
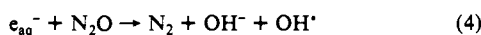
**Irradiations.** The pulse radiolysis experiments were carried out with 0.2–1.5-$\mu$s pulses with 200-mA current of 5-MeV electrons from the linear accelerator at The Hebrew University of Jerusalem. Irradiations were carried out in a 4-cm Spectrosil cell using three light passes. A 150-W xenon lamp produced the analyzing light, and appropriate light filters were used to avoid photochemistry and to eliminate any scattered light. Doses were computed by using $N_2O$-saturated solutions containing 1 mM KSCN and measuring the yield of $(SCN)_2^-$ ($\epsilon_{475}$ = 7600 $M^{-1}$ $cm^{-1}$), assuming a $G$ value of 6. The calculation of absorption coefficients using dosimetry measurements has an error limit of at least 10% due to scatter in the repetition of the pulse intensity and uncertainties in $G$ values. A detailed description of the experimental setup and the techniques used for data analysis has been published previously.[7] Each kinetic run was repeated at least three times, and analysis of traces was done by the LMS method. The average values thus obtained were used to determine the rate constants according to the relevant rate laws. The error limit in these rate constants was estimated from scatter of the results and plausible systematic errors. Large-dose irradiations (up to $10^5$ rad) for product analysis have been carried out with small cylindrical glass bulbs (12-mL volume) filled with 10 mL of deaerated solutions and sealed with a rubber septum.

**Analysis.** The yield of carbon monoxide and carbon dioxide was determined by a gas chromatograph. The gas samples were taken through the rubber septa with gas-tight syringes and were separated on Poropak Q or molecular sieve columns by a Varian 3700 TCD chromatograph with 30 mL/min helium as carrier gas at 60 °C. The yield of oxalate was determined on a Varian 5000 HPLC in a 100-mm stainless-steel column filled with a Teflon support using 85% acetonitrile in water as eluent.
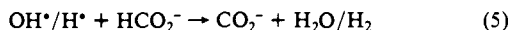
**Production of $CO_2^-$ Radical.** In the irradiation of aqueous solutions, the following radicals are formed:

$$H_2O \rightsquigarrow e_{aq}^- (2.65), OH^\bullet (2.65), H^\bullet (0.6), H_2 (0.45), H_2O_2 (0.75)$$

$$(3)$$
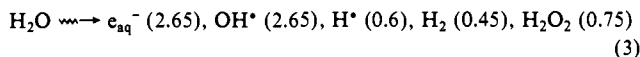
(The numbers in parentheses are the $G$ values, which represent the number of molecules of product formed/100 eV of absorbed energy by the system.)[8] When neutral $N_2O$-saturated solutions ([$N_2O$] = 0.022 M) containing formate ions are irradiated, all the primary radicals are converted into $CO_2^-$ radicals according to reactions 4 and 5. The total
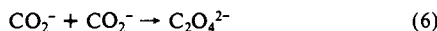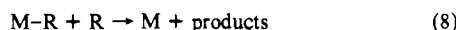
$$e_{aq}^- + N_2O \rightarrow N_2 + OH^- + OH^\bullet$$

$$(4)$$

$$k_4 = 8.7 \times 10^9 \ M^{-1} \ s^{-1} [9]$$

$$OH^\bullet/H^\bullet + HCO_2^- \rightarrow CO_2^- + H_2O/H_2$$

$$(5)$$

$$k_{OH} = 3 \times 10^9 \ M^{-1} \ s^{-1} [10] \qquad k_H = 1.3 \times 10^8 \ M^{-1} \ s^{-1} [11]$$

$G$ value of $CO_2^-$ is 6.1, and in the absence of any other reactants, $CO_2^-$ dimerizes via reaction 6.

$$CO_2^- + CO_2^- \rightarrow C_2O_4^{2-}$$

$$(6)$$

$$2k_6 = 1 \times 10^9 \ M^{-1} \ s^{-1} [12]$$

**Kinetic Evaluations.** When a radical (R) reacts with a metal (M) to form M–R as an intermediate, the latter species may decompose through reaction -7 followed by reaction 8. Assuming a steady-state approximation for [R], rate equation I is obtained. In the presence of an excess

$$M-R \rightleftharpoons M + R$$

$$(-7)$$

$$M-R + R \rightarrow M + \text{products}$$

$$(8)$$

mation for [R], rate equation I is obtained. In the presence of an excess

$$-d[M-R]/dt = 2k_{-7}k_8[M-R]^2/(k_7[M] + k_8[M-R])$$

$$(I)$$

(7) Cohen, H.; Meyerstein, D. *Inorg. Chem.* **1974**, *13*, 2434.

(8) Matheson, M. S.; Dorfman, L. M. *Pulse Radiolysis*; MIT Press: Cambridge, MA, 1965.

(9) Anbar, M.; Barbeneck, M.; Ross, A. B. *Natl. Stand. Ref. Data Ser.* (*U.S., Natl. Bur. Stand.*) **1973**, 43.

(10) Dorfman, L. M.; Adams, G. E. *Natl. Stand. Ref. Data Ser.* (*U.S. Natl. Bur. Stand.*) **1975**, 46.

(11) Anbar, M.; Farhataziz; Ross, A. B. *Natl. Stand. Ref. Data Ser.* (*U.S. Natl. Bur. Stand.*) **1975**, 51.

(12) Ross, A. B.; Neta, P. *Natl. Stand. Ref. Data Ser.* (*U.S. Natl. Bur. Stand.*) **1982**, 70.
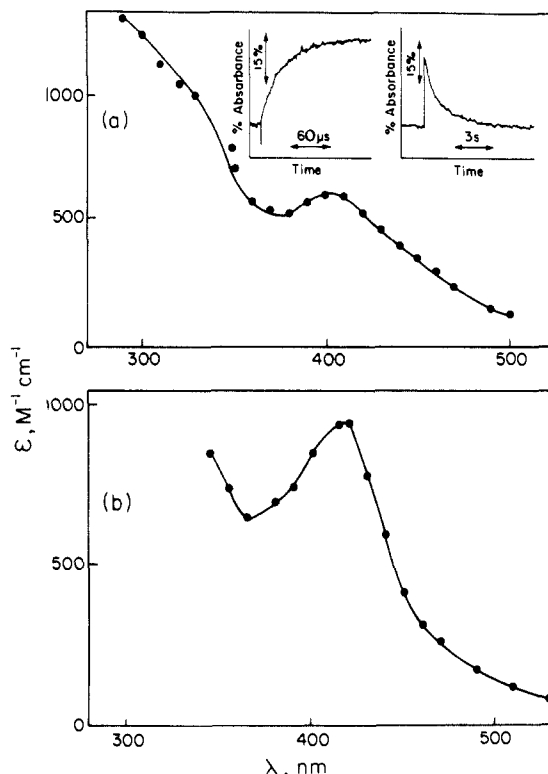
**Figure 1.** Transient spectra formed by the reaction of L–$Fe^{II}$ with $CO_2^-$ at pH 7 in $N_2O$-saturated solutions containing 0.1 M formate. The pulse duration was 0.5 $\mu$s and the optical path length 12.1 cm. Parts: (a) 6 mM NTA, 0.9 mM $FeSO_4$; (b) 3 mM HEDTA, 2 mM $Fe(NH_4)_2(SO_4)_2$·$6H_2O$. The inset in (a) contains typical absorption traces of the formation and decomposition of the transient at 410 nm in $N_2O$-saturated solution at pH 7 containing 4 mM $Fe^{II}$, 6 mM NTA, and 0.1 M formate.

of a radical scavenger (S), where reaction 9 competes efficiently with reaction 8, the M–R intermediate will decompose through reaction -7

$$M-R \rightleftharpoons M + R$$

$$(-7)$$

followed by reaction 9. Assuming again a steady-state approximation

$$R + S \rightarrow \text{products}$$

$$(9)$$

for [R], rate equation II is obtained.

$$-d[M-R]/dt = k_{-7}k_9[S][M-R]/(k_7[M] + k_9[S])$$

$$(II)$$

## Results

$N_2O$-saturated solutions containing 0.03–0.3 M sodium formate, 0.1–4 mM ferrous sulfate or ferrous ammonium sulfate, and 0.1–6 mM L (NTA or HEDTA) in the range pH 4–11 were irradiated. The formation of an absorption between 300 and 600 nm was observed with rates obeying pseudo-first-order kinetics. We attribute this absorption to the formation of the unstable metal-carbon intermediates ($H_2O$)(NTA)$Fe^{III}CO_2^{2-}$ and (HEDTA)-$Fe^{III}CO_2^{2-}$. The spectra of these intermediates as well as a typical kinetic trace are given in Figure 1. The spectra have a maximum absorption band at 405 nm ($\epsilon$ = 620 ± 50 $M^{-1}$ $cm^{-1}$) and at 420 nm ($\epsilon$ = 950 ± 100 $M^{-1}$ $cm^{-1}$) for NTA and HEDTA, respectively. The existence of a second absorption band in the UV region ($\lambda$ ≤ 300 nm), with a much higher extinction coefficient, is indicated by the results. It was impossible to follow the formation of the absorbance at $\lambda$ < 300 nm, since the iron poly(amino carboxylate) complexes absorb very strongly in this region. The molar extinction coefficients were calculated from the absorbance measurements, taking into account the competition by the dimerization reaction of $CO_2^-$ (reaction 6). Some typical results of the observed rates of formation for different [$Fe^{II}$], [$HCO_2^-$], [L], pH, pulse intensity, and wavelengths are summarized in Table I. The formation rates of the unstable intermediates depend on [$Fe^{II}$] and are independent of all other parameters listed above. The absorption disappears with kinetics obeying a second-order rate

**Table I.** Observed Rate Constants of the Formation ($k_f$) and the Decomposition ($k_d$) of the Complexes with the Iron–Carbon $\sigma$-Bond as a Function of Various Conditions

| [$Fe^{II}$], mM | pH | [L], mM | [$HCO_2^-$], M | $k_f$, $s^{-1}$ | $k_d/\epsilon l$, $s^{-1}$ | $\lambda$, nm |
|---|---|---|---|---|---|---|
| | | | Condition A[a] | | | |
| 0.4 | 7 | 6.0 | 0.1 | $7.3 \times 10^3$ | 200 | 410 |
| 0.9 | 7 | 6.0 | 0.1 | $1.9 \times 10^4$ | 59 | 410 |
| 2.0 | 7 | 6.0 | 0.1 | $3.8 \times 10^4$ | 35 | 410 |
| 3.0 | 7 | 6.0 | 0.1 | $4.1 \times 10^4$ | 25 | 410 |
| 4.0 | 7 | 6.0 | 0.1 | $6.7 \times 10^4$ | 20 | 410 |
| 1.0 | 7 | 3.0 | 0.1 | $2.3 \times 10^4$ | 53 | 410 |
| 1.0 | 7 | 1.5 | 0.1 | $2.2 \times 10^4$ | 58 | 410 |
| 1.0 | 7 | 6.0 | 0.03 | $2.0 \times 10^4$ | 58 | 410 |
| 1.0 | 7 | 6.0 | 0.3 | $2.2 \times 10^4$ | 54 | 410 |
| 1.0 | 7 | 6.0 | 0.1 | $2.0 \times 10^4$ | 100 | 480 |
| 1.0 | 5 | 6.0 | 0.1 | $2.2 \times 10^4$ | 45 | 410 |
| 1.0 | 10 | 6.0 | 0.1 | $1.0 \times 10^4$ | 200 | 410 |
| | | | Condition B[b] | | | |
| 1.0 | 7 | 1.5 | 0.1 | $1.1 \times 10^4$ | 4.1 | 420 |
| 1.0 | 7 | 6.0 | 0.1 | $1.2 \times 10^4$ | 3.7 | 420 |
| 2.0 | 7 | 3.0 | 0.1 | $1.9 \times 10^4$ | 1.6 | 420 |
| 2.0 | 7 | 3.0 | 0.1 | $2.1 \times 10^4$ | 4.5 | 460 |
| 3.0 | 7 | 6.0 | 0.1 | $3.1 \times 10^4$ | 1.3 | 420 |
| 4.0 | 7 | 6.0 | 0.1 | $4.0 \times 10^4$ | 0.9 | 420 |

[a] L = NTA, $Fe^{II}$ = $FeSO_4$, $\epsilon$ = 620 $M^{-1}$ $cm^{-1}$, $l$ = 12.1 cm, 0.5-$\mu$s pulse duration. [b] L = HEDTA, $Fe^{II}$ = $Fe(NH_4)_2(SO_4)_2$, $\epsilon$ = 950 $M^{-1}$ $cm^{-1}$, $l$ = 12.1 cm, 0.5-$\mu$s pulse duration.

**Table II.** Observed Rate Constant of the Decomposition ($k_d$) of the Complexes with the Iron–Carbon $\sigma$-Bond in the Presence of $Co(NH_3)_6^{3+}$ or L-$Fe^{III}$ (S)[a]

| NTA | | | HEDTA | | |
|---|---|---|---|---|---|
| [$Fe^{II}$], mM | [S], mM | $k_d$, $s^{-1}$ | [$Fe^{II}$], mM | [S], mM | $k_d$, $s^{-1}$ |
| | | $Co(NH_3)_6^{3+}$ | | | |
| 1.0 | 2.5 | 100 | 1.0 | 0.1 | 9.6 |
| 1.0 | 0.4 | 79 | 1.0 | 0.2 | 14 |
| 1.0 | 0.2 | 43 | 1.0 | 0.4 | 18 |
| 1.0 | 0.1 | 30 | 1.0 | 0.6 | 20 |
| 1.0 | 0.07 | 20 | 0.5 | 0.1 | 14 |
| 0.4 | 0.4 | 110 | 2.0 | 0.1 | 6 |
| 2.0 | 0.4 | 64 | 4.0 | 0.1 | 3.7 |
| 4.0 | 0.4 | 33 | | | |
| | | L-$Fe^{III}$ | | | |
| 1.0 | 0.05 | 22 | 1.0 | 0.02 | 7.3 |
| 1.0 | 0.1 | 40 | 1.0 | 0.04 | 8.3 |
| 1.0 | 0.2 | 67 | 1.0 | 0.08 | 14 |
| 1.0 | 0.4 | 91 | 1.0 | 0.2 | 20 |

[a] Irradiations were carried out in $N_2O$-saturated solutions at pH 7 containing 0.1 M formate and 6 mM L. The decay was followed at 410 and 420 nm for NTA and HEDTA, respectively.

law, and the rate depends on the pH and on the inverse of [L-$Fe^{II}$] (Table I).

Final product analysis was carried out in $N_2O$-saturated solutions containing 4 mM $Fe^{II}$, 6 mM L, and 0.1 M formate at pH 7 irradiated with 80 pulses of $10^3$ rad/pulse. GC and HPLC analyses have shown equal amounts of CO and $CO_2$ and no oxalate. Blank solutions without $Fe^{II}$ showed only oxalate as a final product.

Most of our experiments were carried out at neutral pH, as this pH is the relevant one in biological systems.

Upon the addition of $Co(NH_3)_6^{3+}$ to $N_2O$-saturated solutions containing 6 mM L, 0.2–4 mM $Fe^{II}$, and 0.1 M formate at pH 7, a change in the kinetics from second order to first order was observed. The rate of the disappearance of the absorption increased, and it depended on [$Co(NH_3)_6^{3+}$] and [$Fe^{II}$] (Table II).

During the first and second pulse, in the absence of $Co(NH_3)_6^{3+}$, some bleaching of the signal around 400 nm was observed. This bleaching was attributed to the reaction of $CO_2^-$ with impurities of L-$Fe^{III}$; as in subsequent pulses, no bleaching was observed. In order to measure the rate of the reaction of $CO_2^-$ with L-$Fe^{III}$, we added 0.03–0.2 mM L-$Fe^{III}$ to the L-$Fe^{II}$ solutions containing 0.1 M formate and 6 mM L at pH 7 and observed a bleaching around 400 nm followed by a large increase in the rate of the absorption disappearance and a change in the rate law from
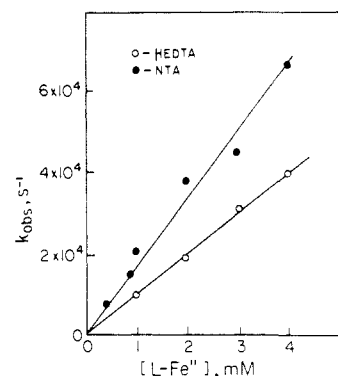


**Figure 2.** Observed rate constant of the formation of the metal–carbon $\sigma$-bonds as a function of [L-$Fe^{II}$] at pH 7 in $N_2O$-saturated solutions containing 0.1 M formate and 6 mM L: ●, L = NTA; O, L = HEDTA.

second-order to first-order kinetics. The results are summarized in Table II. This method for determining the specific rate of the reaction of $CO_2^-$ with L-$Fe^{III}$ was used since L-$Fe^{III}$ absorbs very strongly at 300–400 nm. Therefore, it was impossible to follow the decrease in the absorption of L-$Fe^{III}$ directly under the condition where [L-$Fe^{III}$] $\gg$ [$CO_2^-$].

**Discussion**

The major reactive species present in the solution immediately (1.5 $\mu$s) after the pulse is the $CO_2^-$ radical. As blank solutions without $Fe^{II}$ showed no absorption change, the absorption formed in the presence of $Fe^{II}$ must be due to the reaction product of $CO_2^-$ with the iron(II)–poly(amino carboxylate) complex. The absorption spectra are similar to that of the known $(H_2O)(NTA)Fe^{III}CH_3^-$ complex,[13] their formation obeyed a pseudo-first-order kinetics, and the observed rate constant was linearly dependent on [L-$Fe^{II}$] (Figure 2). We conclude that the absorption observed is due to the formation of $(H_2O)$-$(NTA)Fe^{III}CO_2^{2-}$ and $(HEDTA)Fe^{III}CO_2^{2-}$ (denoted by L-$Fe^{III}CO_2^{2-}$) via eq 10. From the slope of the lines in Figure 2, we determined $k_{10}$ = (1.7 ± 0.3) × $10^7$ and (1.0 ± 0.2) × $10^7$ $M^{-1}$ $s^{-1}$ for NTA and HEDTA, respectively.

$$L-Fe^{II} + CO_2^- \rightarrow L-Fe^{III}CO_2^{2-} \qquad (10)$$
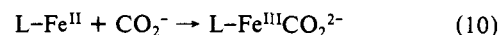
The observed rate of the decomposition of L-$Fe^{III}CO_2^{2-}$ obeyed a second-order rate law. The observed second-order rate constant

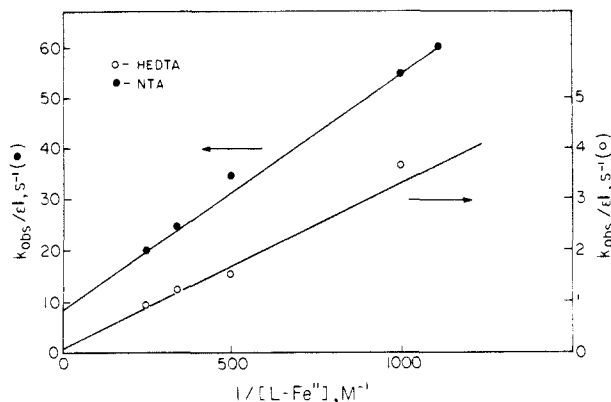(13) Cohen, H.; Meyerstein, D., submitted for publication in *J. Chem. Soc., Dalton Trans.*

**Figure 3.** Dependence of the observed rate constant on the decomposition of the intermediate with the iron–carbon σ-bond versus $1/[L-Fe^{II}]$ at pH 7 in $N_2O$-saturated solutions containing 0.1 M formate and 6 mM L. The pulse intensity was 0.5 μs and the optical path length 12.1 cm. Key: ●, L = NTA; O, L = HEDTA.
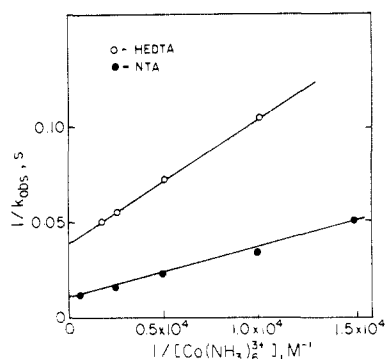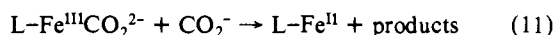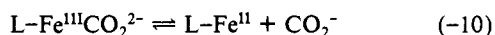


**Figure 4.** Reciprocal of $k_{obsd}$ of the decay of the complex with the metal–carbon σ-bond as a function of $1/[Co(NH_3)_6^{3+}]$ at pH 7 in $N_2O$-saturated solutions containing 6 mM L, 1 mM $FeSO_4$, and 0.1 M formate: ●, L = NTA; O, L = HEDTA.

depended linearly on the inverse of $[L-Fe^{II}]$ (Figure 3) and was independent of the ligand and formate concentrations (Table I). Thus, our observations can be described by the following mechanism:

$$L-Fe^{III}CO_2^{2-} \rightleftharpoons L-Fe^{II} + CO_2^- \qquad (-10)$$

$$L-Fe^{III}CO_2^{2-} + CO_2^- \rightarrow L-Fe^{II} + \text{products} \qquad (11)$$

According to this mechanism rate equation I is valid. Under our experimental conditions, where $k_{10}[L-Fe^{II}] \gg k_{11}[L-Fe^{III}CO_2^{2-}]$, we get eq 12 where $k_{obsd} = 2k_{11}/K_{10}[L-Fe^{II}]$ (Figure 3). As can

$$-d[L-Fe^{III}CO_2^{2-}]/dt = 2k_{11}[L-Fe^{III}CO_2^{2-}]^2/K_{10}[L-Fe^{II}]$$
$$= k_{obsd}[L-Fe^{III}CO_2^{2-}]^2 \qquad (12)$$

be seen, a good linear correlation is obtained. From the slopes (Figure 3), the values of $k_{11}/K_{10} = 175 \pm 30$ and $18 \pm 2$ s$^{-1}$ can be obtained for NTA and HEDTA, respectively. The intercepts of the lines differ from zero as the dimerization reaction of $CO_2^-$ cannot be neglected under the experimental conditions.

In order to determine $K_{10}$, we added a $CO_2^-$ scavenger (Co-$(NH_3)_6^{3+}$) to the solutions so that reaction 13 would compete

$$Co(NH_3)_6^{3+} + CO_2^- \rightarrow Co(NH_3)_6^{2+} + CO_2 \qquad (13)$$
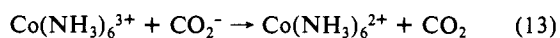
$$k_{13} = 4 \times 10^7 \text{ M}^{-1} \text{ s}^{-1\,14}$$

efficiently with reaction 11 and the disappearance of the transient with the iron–carbon σ-bond would obey rate equation II. Rearrangement of equation II yields eq 14. In Figure 4 the re-

$$1/k_{obsd} = 1/k_{-10} + K_{10}[L-Fe^{II}]/k_{13}[Co(NH_3)_6^{3+}] \qquad (14)$$

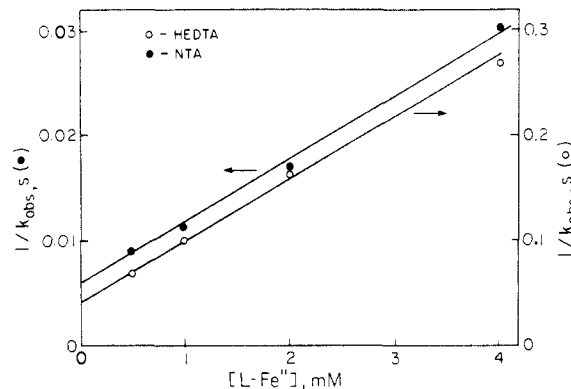(14) Cohen, H.; Meyerstein, D. *J. Am. Chem. Soc.* **1972**, *94*, 6944.



**Figure 5.** Reciprocal of $k_{obsd}$ of the decay of the complex with the metal–carbon σ-bond as a function of $[L-Fe^{II}]$ at constant concentration of $Co(NH_3)_6^{3+}$ at pH 7 in $N_2O$-saturated solutions containing 6 mM L and 0.1 M formate: ●, L = NTA, $[Co(NH_3)_6^{3+}] = 0.4$ mM; O, L = HEDTA, $[Co(NH_3)_6^{3+}] = 0.1$ mM.

**Table III.** Specific Rates of the Reactions of Formation and Decomposition of the Iron–Carbon σ-Bonds

| | L | |
|---|---|---|
| specific rates | NTA | HEDTA |
| $k_{10}$, M$^{-1}$ s$^{-1}$ | $1.5 \times 10^7$ | $6.2 \times 10^6$ |
| $k_{-10}$, s$^{-1}$ | 140 | 25 |
| $K_{10}$, M$^{-1}$ | $1.1 \times 10^5$ | $2.5 \times 10^5$ |
| $k_{11}$, M$^{-1}$ s$^{-1}$ | $1.9 \times 10^7$ | $4.5 \times 10^6$ |
| $k_{15}$, M$^{-1}$ s$^{-1}$ | $5.5 \times 10^7$ | $8.3 \times 10^7$ |

ciprocal of $k_{obsd}$ is plotted versus $1/[Co(NH_3)_6^{3+}]$ at constant $[L-Fe^{II}]$ and in Figure 5 versus $[L-Fe^{II}]$ at constant $[Co-(NH_3)_6^{3+}]$. From the slopes of these lines, we determined $K_{10} = (1.1 \pm 0.1) \times 10^5$ and $(2.5 \pm 0.1) \times 10^5$ M$^{-1}$ for NTA and HEDTA, respectively. From the intercepts of these lines, we obtained $k_{-10} = 130 \pm 30$ and $25 \pm 2$ s$^{-1}$ for NTA and HEDTA, respectively. The specific rates of the formation of the complexes with the iron–carbon σ-bond ($k_{10}$) can also be calculated, and the values obtained are $(1.5 \pm 0.5) \times 10^7$ and $(6.2 \pm 0.6) \times 10^6$ M$^{-1}$ s$^{-1}$ for NTA and HEDTA, respectively, which are in good agreement with those determined directly. Knowing the values of $K_{10}$, we calculated from the slopes of the lines in Figure 3 $k_{11} = (1.9 \pm 0.4) \times 10^7$ and $(4.5 \pm 0.2) \times 10^6$ M$^{-1}$ s$^{-1}$ for NTA and HEDTA, respectively.

Upon addition of $L-Fe^{III}$ as a scavenger (instead of $Co-(NH_3)_6^{3+}$), the rate of reaction 15 could be determined (using the

$$L-Fe^{III} + CO_2^- \rightarrow L-Fe^{II} + CO_2 \qquad (15)$$
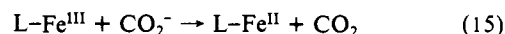
same plots as those in Figures 4 and 5). We have found $k_{15} = (5.5 \pm 1.0) \times 10^7$ M$^{-1}$ s$^{-1}$ and $k_{-10} = 170 \pm 20$ s$^{-1}$ for NTA and $k_{15} = (8.3 \pm 0.5) \times 10^7$ M$^{-1}$ s$^{-1}$ and $k_{-10} = 25 \pm 2$ s$^{-1}$ for HEDTA.

The average values of the rate constants calculated for the different reactions by the different methods are summarized in Table III. From the kinetic parameters listed in Table III, some interesting conclusions can be drawn:

(a) Although the $CO_2^-$ is a strong reducing agent, it does not reduce the ferrous poly(amino carboxylate) complexes as it does the corresponding ferrous protoporphyrin[15] but rather forms a metal–carbon σ-bond. The formation of analogous transients was observed when $CO_2^-$ reacts with $Cr_{aq}^{2+}$,[16] $Cu_{aq}^+$,[17] and $Co^{II}$-$(NTA)(H_2O)_2^-$.[18]

(b) The specific rate constant of reaction 10 is by a factor of 2 larger for the ferrous NTA complex, which has two cis water positions that can exchange the water with the $CO_2^-$ as compared

(15) Sorek, Y.; Cohen, H.; Meyerstein, D. *J. Chem. Soc., Faraday Trans. 1* **1985**, *81*, 233.

(16) Ellis, D.; Green, M.; Sykes, A. G.; Buxton, G. V.; Sellers, R. M. *J. Chem. Soc., Dalton Trans.* **1973**, 1724.

(17) Das, S.; Johnson, J. R. *J. Chem. Soc., Faraday Trans. 1* **1980**, *74*, 1779.

(18) Meyerstein, D.; Schwarz, H. A *J. Chem. Soc. Faraday Trans 1*, in press.

to the single aquo ligand for the HEDTA complex. This is in accord with the expectation for an inner-sphere mechanism, which clearly is required for the formation of the Fe–C bond.

(c) The stability constants of the ferric–carbon entities are large, $K_{10} \sim 10^5$ M$^{-1}$. Thus, the overall free energy gains for reaction 10 are 6.9 and 7.3 kcal/mol for NTA and HEDTA, respectively. It is interesting to note that the corresponding equilibrium constant for the formation of (H$_2$O)NTA–Fe$^{III}$CH$_3^-$ is lower, 2.5 × 10$^3$ M$^{-1}$.[13] This result indicates that the iron–carbon bond in L–Fe$^{III}$CO$_2^{2-}$ is stronger than in L–Fe$^{III}$CH$_3^-$.

The results obtained for the ferrous HEDTA complex show that the intermediate observed by Rush and Koppenol[6] (upon mixing this complex with H$_2$O$_2$ in the presence of formate) is not the suggested Fe$^{II}$HEDTA• ligand radical (formed from the decomposition of the ternary complex of the ferrous–peroxo complex with formate) but the complex with the metal–carbon σ-bond. This conclusion results from the fact that both the absorption spectrum and their reported kinetics agree well with our observation for the HEDTA–Fe$^{III}$CO$_2^{2-}$. The HEDTA–Fe$^{II}$ possibly reacts with H$_2$O$_2$ to yield either the OH• radical or the HEDTA–Fe$^{II}$H$_2$O$_2$ complex, which subsequently reacts with excess concentration of HCO$_2^-$ via reaction 16. The CO$_2^-$ radical

$$OH^\bullet/L\text{–}Fe^{II}H_2O_2 + HCO_2^- \rightarrow H_2O/L\text{–}Fe^{III} + CO_2^- \quad (16)$$

produced reacts via reactions 10 and 11. Taking the concentrations used by Rush and Koppenol[6] and the known specific rate constants of the relevant reactions, the calculations show that in their experiments the HEDTA–Fe$^{III}$CO$_2^{2-}$ was formed within the mixing time of HEDTA–Fe$^{II}$ with H$_2$O$_2$ in the presence of formate.

It is interesting to note that the decomposition reaction (11) at pH 7, which involves the attack of CO$_2^-$ on the Fe$^{III}$CO$_2^{2-}$ complex, yields equimolar concentrations of CO$_2$ and CO in

contrast to the bimolecular reaction of CO$_2^-$ in the absence of L–Fe$^{II}$, which yields oxalate anion. The iron complex thus acts as a catalyst for the disproportionation reaction (eq 17). The

$$L\text{–}Fe^{III}CO_2^{2-} + CO_2^- + 2H^+ \rightarrow L\text{–}Fe^{II} + CO + CO_2 + H_2O \quad (17)$$
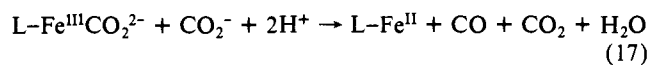
data are insufficient for a detailed analysis of the mechanism of this reaction, which is probably a model reaction to processes occurring in the catalytic reduction of CO$_2$, e.g. in electrocatalytic processes.[19]

It would be very interesting to study the same system with more complicated carbon radicals, e.g. glycerol, ribose, ATP, etc., and to see whether in these systems degradation of the ligand would be the result of the decomposition reaction of the metal–carbon complex. These systems might serve as a model for biological damage, where, through an intermediate with a metal–carbon σ-bond, the damage occurs site specifically.

(19) Beley, M.; Collin, J. P.; Rupert, R.; Sauvage, J. P. *J. Am. Chem. Soc.* **1986,** *108,* 7461.

# Anisotropic Exchange in the Co₂(EDTA)·6H₂O and CoCu(EDTA)·6H₂O Bimetallic Ordered Chains. Low-Temperature Investigation of the Thermal and Magnetic Properties

**E. Coronado,**[†,§,1] **M. Drillon,**[*,†] **P. R. Nugteren,**[‡] **L. J. de Jongh,**[‡] **and D. Beltran**[§]

*Contribution from the Département Science des Matériaux-EHICS, 1, rue B. Pascal 67008, Strasbourg, France, Kamerlingh Onnes Laboratorium, Leiden University, P.O. Box 9506, 2300 Ra Leiden, The Netherlands, Departamento de Quimica Inorganica, Burjasot, Valencia, Spain. Received August 28, 1987*

**Abstract:** We report on the thermal and magnetic behaviors of the chain complexes Co₂(EDTA)·6H₂O and CoCu(EDTA)·6H₂O characterized by two different sites for the metal ions. These are octahedrally coordinated either to EDTA ligands or to oxygen atoms of carboxylate groups and four water molecules in order to form alternating zigzag chains. The thermodynamic properties (EPR, high field magnetization, specific heat, and magnetic susceptibility) are discussed in terms of an Ising chain model with regularly or alternatingly spaced sites. It is emphasized, for the first time, that the different $g$ values at different (alternating) sites give rise to a ferrimagnetic-like behavior even for a large dimerization of the chains.

Recently, much experimental and theoretical effort has been devoted to the properties of ordered bimetallic systems, in particular to what is currently referred to as 1d ferrimagnets.[2–9] These may be defined as two sublattice chains in which one sublattice does not compensate the other, due to different spins or also to different coordination environments for the metal ions on each sublattice. Several physical situations, related to real

systems, have been considered and solved rigorously. Thus, closed-form expressions of the thermodynamic quantities of interest

† Département Science des Materiaux-EHICS.
‡ Kamerlingh Onnes Laboratorium.
§ Departamento de Quimica Inorganica.

(1) Permanent address: Departamento de Quimica Inorganica, Valencia, Spain.

(2) Drillon, M.; Coronado, E.; Beltran, D.; Curely, J.; Georges, R.; Nugteren, P. R.; de Jongh, L. J.; Genicon, J. L. *J. Magn. Magn. Mater.* **1986,** *54–57,* 1507.

(3) Drillon, M.; Coronado, E.; Beltran, D.; Georges, R. *J. Appl. Phys.* **1985,** *57,* 3353.

(4) Coronado, E.; Drillon, M.; Fuertes, A.; Beltran, D.; Mosset, A.; Galy, J. *J. Am. Chem. Soc.* **1986,** *108,* 900 and references therein.